Journal of Intelligent & Robotic Systems (2024) 110:43
https://doi.org/10.1007/s10846-024-02076-5

REGULAR PAPER

A Novel Communication Time-Delay Cooperative Control Method with Switching Event-Triggered Strategy

Dongni Li[1] · Liang Cao[2] · Yingnan Pan[1] · Wenbin Xiao[3] · Hong Xue[2]

Received: 7 July 2023 / Accepted: 21 February 2024 / Published online: 11 March 2024

Abstract
A novel communication time-delay classification-based method is designed for nonlinear multiagent systems with the finite-time prescribed performance function. The time-delay phenomenon for communication channels between agents is discussed. Then, an improved time-delay classification method is proposed to broaden the standard of classification mechanism by considering the degree of deviation and relative variation of neighbor agents, rather than classifying the delay time into large time-delay and small time-delay. Based on this, the unified Lyapunov-Krasovskii functional and the finite-time performance function are used to solve the large time-delay phenomenon and ensure that the error is within the preset boundary, respectively. Furthermore, a modified switching event-triggered strategy is put forward to reduce the transmission burden, which considers the impact of tracking error to adjust the threshold condition in real-time. Additionally, all signals of the closed-loop systems are bounded. Eventually, two simulation examples verify the validity of the control strategy.

Keywords Communication time-delay classification-based method · Finite-time performance function · Switching event-triggered strategy · Nonlinear multiagent systems

1 Introduction

The cooperative control schemes for multiagent systems (MASs) [1–12] have been broadly discussed over the past few years. To achieve the consensus control objective between the leader and followers, the tracking control is an important work for MASs. For example, the authors introduced a neural-network-based adaptive controller to fulfill the objective of asymptotically consensus control for nonlinear MASs [13]. To carry out the tracking control scheme, Zhang et al. explored the adaptive controller, which is based on FLSs for MASs subject to unknown disturbances [14]. By designing an adaptive neural backstepping approach, Shang et al. [15] addressed the consensus control problem by using the backstepping technology for distributed nonlinear MASs. However, the above achievements [13–15] finish the target of tracking control through the complex network, which do not take into account the impact of the time-delay phenomenon.

Time delays cause information interactions to be unsynchronized and do not accomplish the intended control objectives [16, 17]. Over the years, the time-delay phenomenon has been exhaustively investigated for MASs. In [18], time delays were classified into large time-delay and small time-delay. However, the above method takes the same classification method for time delays that occur in arbitrary links, which is not very reasonable. Furthermore, many meaningful results have been made for time-delay phenomenon on different communication links. In [19], the authors considered the impact of the state time-delay on nonlinear MASs. Ma et al.

✉ Liang Cao
caoliang0928@163.com

Dongni Li
lidongni1999@163.com

Yingnan Pan
panyingnan0803@gmail.com

Wenbin Xiao
xiaowb992@163.com

Hong Xue
xuehong19870101@163.com

[1] College of Control Science and Engineering, Bohai University, Jinzhou, Liaoning 121013, People's Republic of China

[2] College of Mathematical Sciences, Bohai University, Jinzhou, Liaoning 121013, People's Republic of China

[3] School of Information and Electrical Engineering, Hunan University of Science and Technology, Xiangtan, Hunan 411201, People's Republic of China

[20] investigated the asymptotic tracking control issue for nonlinear time-delay systems. The time-delay results in [19] and [20] consider the problem of state delays. There is little research on consensus control of MASs with communication time-delay, which is a necessary link for agents to achieve control objectives. This motivates us to study the time-delay in communication channels between agents for MASs. Therefore, it is significant to investigate the different classification methods for different time delays and alleviate the effects of time delays. Meanwhile, in the domain of control theory and its practical applications, the prescribed performance control design algorithm has been developed to preset the transient and steady state performances of dynamic systems. Liu et al. first proposed the finite-time performance function (FTPF) in [21], which guaranteed the tracking error within a preconditioned range and enabled results curves with transient response. Sui et al. [22] investigated a new control scheme for constraint nonlinear systems with FTPF. While the above results effectively keep system performance, there are still certain difficulties in applying FTPF to MASs. However, it is worth investigating how to use the FTPF to ensure that nonlinear MASs with communication time delays are stable for a predetermined period of time.

To accomplish the desired control goals, information transfer between multiple agents often requires a large amount of communication, which leads to a certain network burden. Quantization and event-triggered (ET) mechanism are widely used as the main means to effectively solve the problem of communication burden. The control signal would usually be quantized before being transmitted over the communication channel. Quantization has an impact on system performance inevitably, which has aroused widespread concern. In [23], the control signal was quantized for nonlinear networked systems. The authors [24] used quantitative signals to get the goal of saving communication resources for MASs. At the same time, because MASs require extensive communication to achieve information interaction, the network burden needs to be reduced. The ET strategy has been investigated in [25–30]. For example, the authors designed a switching threshold ET strategy to reduce the transmission load in [31]. Pang et al. [32] proposed the adaptive cooperative control method of nonlinear systems with the switching ET threshold. Wang et al. [33] designed the switching ET control scheme for nonlinear MASs subject to sensor faults. However, the above switching threshold ET mechanisms [31–33] ignore the tracking performance metrics of the system to adjust the ET threshold. Hence, establishing both ET mechanism and quantization strategy to further address the communication burden of MASs remains a challenging topic.

In light of the above considerations, a novel communication channels time-delay classification-based method is designed for MASs with modified switching ET strategy. Meanwhile, considering both quantization and ET mechanism can further address the communication burden. The dominant contributions and features of this paper would be synthesized as follows:

1) A novel time-delay classification-based method is proposed to better describe small time-delay and large time-delay for communication links, which considers the deviation between neighbor agents and reference signal to design the classification condition. According to the synchronization of agents, appropriate confidence intervals are taken to form another standard for classification.
2) With the help of the unified Lyapunov-Krasovskii functional and the finite-time performance function, the large time-delay phenomenon is solved and the error is ensured within the preset boundary, respectively. The designed control algorithm achieves the consensus control objective of agents in finite time.
3) Different from the existing switching ET mechanisms, the tracking error is set to design the switching rules of switching ET mechanism. When the tracking error becomes larger or smaller, the update frequency of the system should be appropriately increased or reduced. The threshold strategy is used to achieve the appropriate update of the control signal through user-defined threshold conditions.

The organization of this paper is shown below. Section 2 explicitly provides the preliminary knowledge. To acquire the control objectives, the designed controller is displayed in Section 3. Furthermore, Section 4 fulfills the stability analysis. Simulation results certify the applicability of the designed control strategy in Section 5. Section 6 provides a description of the conclusions.

2 Preliminaries

2.1 Graph Theory

The direction of information transmission between agents can be shown by a directed graph. A directed graph is denoted as $\mathcal{G} = (\mathcal{V}, \mathcal{E})$ to describe a set of agents. $\mathcal{V} = (1, \ldots, N)$ is a nonempty set of nodes. $\mathcal{E} \subseteq \mathcal{V} \times \mathcal{V}$ means the set of edges. Meanwhile, the definition of $(\mathcal{V}_i, \mathcal{V}_\pi) \in \mathcal{E}$ exists the edge of node π to node i, and the agent i obtains the information from π. Furthermore, $\mathcal{A} = \left[a_{i,\pi}\right] \in \mathbb{R}^{N\times N}$ represents the relevant adjacency matrix. If i obtains the information from π, $a_{i,\pi} > 0$. Else, $a_{i,\pi} = 0$. Furthermore, $\mathcal{D}$ means the diagonal matrix, where $\mathcal{D} = \text{diag}\,(d_1, \ldots, d_N)$ with $d_i = \sum_{\pi=1}^{N} a_{i,\pi}$. The Laplacian matrix is denoted as $\mathcal{L}$ with $\mathcal{L} = \mathcal{D} - \mathcal{A}$.

Assumption 1 [1] *If there exists at least one directed path from the root node to all other nodes, then $\mathcal{G}$ has a spanning tree with $\boldsymbol{0}$ as the root node.*

Assumption 2 [1] *Based on the backstepping technique, the reference signal y_r and its first-order derivative are required to be bounded for the tracking control problem. Meanwhile, the disturbance term is bounded with $d_{i,f} \leq d_{i,f}^*$.*

2.2 Problem Formulation

The dynamic of the ith ($i = 1, \ldots, N$) agent is given by

$$\begin{cases} \dot{x}_{i,\iota} = x_{i,\iota+1} + F_{i,\iota}(\bar{x}_{i,\iota}) + \varpi_{i,\iota} \\ \dot{x}_{i,n} = Q_i(u_i) + F_{i,n}(\bar{x}_{i,n}) + \varpi_{i,n} \\ y_i = x_{i,1} \end{cases} \tag{1}$$

where $\bar{x}_{i,\iota} = [x_{i,1}, x_{i,2}, \ldots, x_{i,\iota}]^T \in \mathbb{R}^\iota$ and $\bar{x}_{i,n} = [x_{i,1}, x_{i,2}, \ldots, x_{i,n}]^T \in \mathbb{R}^n$ show the state vectors with $\iota = 1, \ldots, n-1$. The quantified input signal is expressed as $Q_i(u_i)$. The output signal of the ith agent is represented as y_i. Unknown nonlinear functions are indicated as $F_{i,\iota}(\bar{x}_{i,\iota})$ and $F_{i,n}(\bar{x}_{i,n})$. External disturbances are considered as $\varpi_{i,\iota}$ and $\varpi_{i,n}$.

Lemma 1 [34] *Define $\mathcal{B} = diag\{b_i\} \in \mathbb{R}^{N\times N}$, where $b_i > 0$ for at least one i. Then, $\mathcal{L} + \mathcal{B}$ is nonsingular.*

Lemma 2 [34] *Define $s_{.1} = (s_{1,1}, s_{2,1}, ..., s_{N,1})^T$, $y = (y_1, y_2, ..., y_N)^T$ and $y_r^* = (y_r, y_r, ..., y_r)^T$, the next inequality holds*

$$|| \, y - y_r^* \, || \leq \frac{|| \, s_{.1} \, ||}{\sigma(\mathcal{L} + \mathcal{B})}, \tag{2}$$

where $\sigma(\mathcal{L} + \mathcal{B})$ represents the minimum singular value of $\mathcal{L} + \mathcal{B}$.

Lemma 3 [34] *Define $\omega = [\omega_1, \omega_2, \ldots, \omega_n]^T$ and $\delta(x) = [\delta_1(x), \ldots, \delta_n(x)]^T$, it can be shown as*

$$y(x) = \omega^T \delta(x). \tag{3}$$

The fuzzy logic systems are defined as

$$\sup_{x\in\varkappa} |y(x) - \omega^T \delta(x)| \leq \upsilon, \tag{4}$$

where $y(x)$ is a continuous function with $\upsilon > 0$, and it is defined on a compact set $\varkappa$.

Lemma 4 [35] *The second-order sliding mode integral filter (SSMIF) is characterized as*

$$\begin{cases} \dot{R}_{i,p10} = -\frac{R_{i,p10} - \xi(t)}{\chi_{i,p10}} - \frac{J_{i,p10}(R_{i,p10} - \xi(t))}{\|R_{i,p10} - \xi(t)\| + P_{i,p10}} \\ \dot{R}_{i,p20} = -\frac{R_{i,p20} - \dot{R}_{i,p10}}{\chi_{i,p20}} - \frac{J_{i,p20}(R_{i,p20} - \dot{R}_{i,p10})}{\|R_{i,p20} - \dot{R}_{i,p10}\| + P_{i,p20}}, \end{cases}$$

where $R_{i,p10}$ and $R_{i,p20}$ are the states of the filter. $\chi_{i,p10}$, $\chi_{i,p20}$, $P_{i,p10}$, $P_{i,p20}$, $J_{i,p10}$ and $J_{i,p20}$ are positive parameters. $\xi(t)$ is the known function.

Lemma 5 [36] *There are functions $D_i(u_i)$ and $P_i(t)$ such that the quantized value $Q_i(u_i)$ satisfies*

$$Q_i(u_i) = D_i(u_i)u_i + P_i(t) \tag{5}$$

where

$$D_i(u_i) = \begin{cases} \dfrac{Q_i(u_i)}{u_i}, & |u_i| > u_{i,\min} \\ 1, & |u_i| \leq u_{i,\min} \end{cases} \tag{6}$$

and

$$P_i(t) = \begin{cases} 0, & |u_i| > u_{i,\min} \\ -u_i, & |u_i| \leq u_{i,\min}. \end{cases} \tag{7}$$

The above functions are sufficient for the following requirements

$$\begin{aligned} &1 - \gamma_i \leq D_i(u_i) \leq 1 + \gamma_i \\ &|P_i(t)| \leq u_{i,\min}. \end{aligned} \tag{8}$$

The use of Lemma 1 is to keep the normal communication of MASs, ensuring that each follower can directly or indirectly receive information from the leader. Lemma 2 is used to prove that the consensus tracking errors can converge to a small neighborhood of the origin, and is widely used in adaptive tracking control strategies for MASs. Next, due to the presence of certain unknown nonlinear functions in nonlinear MASs, FLSs are often used to approximate unknown nonlinear terms. Therefore, Lemma 3 is often used by scholars as a tool to approximate unknown nonlinear terms. Finally, with the help of the SSMIF, Lemma 4 is used to avoid the complex process caused by controller derivation. Lemma 5 is necessary when considering input quantization problems, as the quantization problems considered in this paper are divided into four situations. Use Lemma 5 to uniformly represent all occurrences for subsequent theoretical derivation and problem discussion.

2.3 A Novel Delay Classification

In the existing paper [18], the time-delay phenomenon is divided into large time-delay and small time-delay, which is defined according to the step size that the delay time lags behind the current step. In control systems, it is not sufficient to measure time-delay phenomenon only by time, especially when considering communication time delays.

Confidence intervals are the estimated intervals of the population parameters which are constructed from the sample statistics. $\Delta x_{i,1}$ denotes the amount of change in adjacent sampling moments. Consider $\left|\frac{\Delta x_{i,1}}{\Delta x_{\pi,1}}\right|$ as a sample $x_{\pi,1}$ and take a confidence interval of 0.95. Based on this sample, with a given confidence level, a minimum interval can be determined. θ_1 and θ_2 are referred to as the lower and upper confidence limits, respectively. For $[\theta_1, \theta_2]$, one has

$$P\left(\theta_1 \leq \left|\frac{\Delta x_{i,1}}{\Delta x_{\pi,1}}\right| \leq \theta_2\right) = 0.95. \tag{9}$$

In an ideal situation, the amount of change of $x_{i,1}$ will be consistent with the amount of change of $x_{\pi,1}$. According to the probability distribution, the expected value is one. Within the set confidence interval, the delay is classified as the small time-delay periods $\tau_{i,\pi,\min}$. Otherwise, it is considered as the large time-delay periods $\tau_{i,\pi,\max}$. For the confidence interval, one has

$$\begin{aligned}\left|\frac{\Delta x_{i,1}}{\Delta x_{\pi,1}}\right|_1 &= \left\{\bar{x}_{\pi,1} - 1.96\frac{\sigma}{k^{\frac{1}{2}}} \leq x_{\pi,1} \leq \bar{x}_{\pi,1} + 1.96\frac{\sigma}{k^{\frac{1}{2}}}\right\} \\ \left|\frac{\Delta x_{i,1}}{\Delta x_{\pi,1}}\right|_2 &= \left\{x_{\pi,1} > \bar{x}_{\pi,1} + 1.96\frac{\sigma}{k^{\frac{1}{2}}} \vee x_{\pi,1} < \bar{x}_{\pi,1} - 1.96\frac{\sigma}{k^{\frac{1}{2}}}\right\}\end{aligned} \tag{10}$$

where $\left|\frac{\Delta x_{i,1}}{\Delta x_{\pi,1}}\right|_1$ represents within the confidence interval, and $\left|\frac{\Delta x_{i,1}}{\Delta x_{\pi,1}}\right|_2$ means the outside of the confidence interval. The sample size is denoted as k, and the sample variance is shown as σ. The average value of states in the sampling interval is denoted as $\bar{x}_{\pi,1}$.

A new time-delay classification method is proposed, for any time interval $[\gamma_0, \gamma_1)$, the following two sets are designed with $0 \leq \gamma_0 \leq \gamma_1$.

$$\tau_{i,\pi} = \begin{cases} \tau_{i,\pi,\min} & \left|x_{\pi,1} - y_r\right| < M \quad \text{and} \quad \left|\frac{\Delta x_{i,1}}{\Delta x_{\pi,1}}\right|_1 \\ \tau_{i,\pi,\max} & \left|x_{\pi,1} - y_r\right| \geq M \quad \text{or} \quad \left|\frac{\Delta x_{i,1}}{\Delta x_{\pi,1}}\right|_2, \end{cases} \tag{11}$$

where M is a designed constant. The reference signal is denoted as y_r. The degree of deviation from the reference signal is indicated as $\left|x_{\pi,1} - y_r\right|$. If within the preset range, it indicates that it is within a reasonable deviation from the leader, and indicates that the neighbor agent $x_{\pi,1}$ receives information in a timely manner to achieve the consensus on the reference signal.

Algorithm 1 Communication time-delay classification-based cooperative control method.

1: Initialize parameters $x_{i,1}(t_0)$ and $x_{\pi,1}(t_0)$.
2: Set variable y_r and M.
3: Select sampling step size k.
4: Record neighbor status values $x_{\pi,1}$ during sampling time.
5: Calculate the variance σ and average $\bar{x}_{\pi,1}$ of sampled data.
6: **if** $\bar{x}_{\pi,1} - 1.96\frac{\sigma}{k^{\frac{1}{2}}} \leq x_{\pi,1} \leq \bar{x}_{\pi,1} + 1.96\frac{\sigma}{k^{\frac{1}{2}}}$ && $\mid x_{\pi,1} - y_r \mid < M$
7: **then** $\tau_{i,\pi} = \tau_{i,\pi,min}$;
8: **else**
9: **then** $\tau_{i,\pi} = \tau_{i,\pi,max}$;
10: **end**
11: Return Time delays judgment result $\tau_{i,\pi}$.

Remark 1 A novel time-delay classification-based method is designed to better describe small time-delay and large time-delay for communication links, which considers the deviation between neighbor agents and reference signal to design the classification condition. Due to the diverse time-delay situations in the practical control process, it is significant to consider the different classification methods for different time delays and alleviate the effects of time delays.

2.4 Modified Switching Event-Triggered Strategy

A modified switching ET mechanism is designed, which considers the system performance in the current state to select a reasonable ET threshold condition. It is important to balance system performance and controller update times when designing switching conditions. The tracking error is a crucial metric for evaluating the real-time performance of a system. In view of this feature, the tracking error is leveraged to establish switching conditions for selecting the appropriate mechanism. The relative threshold strategy is adopted over the fixed threshold strategy, as it ensures that the threshold is also large when the amplitude of the control signal is large. Hence, the relative threshold strategy is deemed more effective for accurate control of the system, particularly when the tracking error is small or u_i approaches zero. This results in better system performance, stability and lower update frequency.

During the start stage of the control scheme, the system often encounters the negative influence such as jumping and shaking. It will definitely reduce the performance of the system, especially in tracking control. A fixed threshold strategy can be adopted, and the user can adjust the threshold. Based on these analysis, a modified switching ET strategy is

designed as follows:

$$u_i(t) = \vartheta_i(t_{i,\Gamma}), \qquad \forall t \in [t_{i,\Gamma}, t_{i,\Gamma+1}) \tag{12}$$

$$t_{i,\Gamma+1} = \begin{cases} \inf\left\{t \in R \mid \left|E_i(t)\right| \geq \varrho_i \left|u_i(t)\right| + l_{i,1}\right\} & \left|z_{i,n}\right| < \phi_i \\ \inf\left\{t \in R \mid \left|E_i(t)\right| \geq l_{i,2}\right\} & \left|z_{i,n}\right| \geq \phi_i, \end{cases} \tag{13}$$

where $E_i(t)$ is the measurement error with $E_i(t) = \vartheta_i(t) - u_i(t)$. The intermediate signal $\vartheta_i(t)$ is defined in (40). The constants ϱ_i, $l_{i,1}$ and $l_{i,2}$ can be designed, and one has $0 < \varrho_i < 1$. The trigger time for $\Gamma \in Z^+$ is indicated as $t_{i,\Gamma}$. The specific definition of $z_{i,n}$ can be seen in (24). The designed condition of switching threshold is shown as ϕ_i. When choosing the parameter ϕ_i, the communication burden of the system is reduced to a certain extent.

The proposed mechanism enables the user to alter the controller update frequency by manipulating the parameter ϕ_i to attain the desired tracking performance when the tracking metrics are not within the expected range. On the other hand, when the tracking metrics fall within the preset threshold, the ET threshold is achieved by considering the controller value to maximize the communication resource savings. The threshold design strategy outlined encompasses the traits of two ET strategies and confers higher adaptability in maintaining a balance between system performance and communication load.

Remark 2 Different from the existing switching ET mechanisms [31–33], the tracking error is set to design the switching rules of switching ET mechanism. When the tracking error becomes larger or smaller, the update frequency of the system should be appropriately increased or reduced. The fixed threshold ET mechanism is applied to flexibly adjust the number of updates when the error is larger than the designed switching value. Meanwhile, another case is illustrated when the error is smaller than the designed switching value, and the system exists in a relatively more stable state.

2.5 Finite-Time Performance Function

Definition 1 A smooth function $\zeta_i(t)$ is called as the FTPF when it satisfies the following rules:
1) $\zeta_i(t) > 0$ and $\dot{\zeta}_i(t) \leq 0$.
2) $\lim_{t \to T_0} \zeta_i(t) = \zeta_i(T_0)$ which is an arbitrarily small positive constant.
3) $\zeta_i(t) = \zeta_i(T_0)$ for $t \geq T_0$ with T_0 being the settling time.

Based on Definition 1, $\zeta_i(t)$ can be represented as

$$\zeta_i(t) = \begin{cases} (\zeta_{i,0}^{\nu_i} - \nu_i \beta_i t)^{\frac{1}{\nu_i}} + \zeta_i(T_0), & 0 \leq t < T_0 \\ \zeta_i(T_0), & t \geq T_0, \end{cases} \tag{14}$$

where $\zeta_{i,0}$, $\zeta_i(T_0)$, ν_i and β_i are positive constants with $\nu_i = \frac{w_i}{s_i}$. Any positive odd and even integer are defined as w_i and s_i, respectively.

The initial value is denoted as $\zeta_{i,0} + \zeta_i(T_0) = \zeta_i(0)$. The settling time and the maximum allowable size of the tracking error at steady state are indicated as $T_0 = \frac{\zeta_{i,0}^{\nu_i}}{\nu_i \beta_i}$ and $\zeta_i(T_0) = \lim_{t \to T_0} \zeta_i(t)$, respectively.

To get the target of this paper, the following inequality is introduced

$$-\zeta_i(t) < z_{i,1}(t) < \zeta_i(t). \tag{15}$$

The maximum overshoot of the tracking error does not exceed $\zeta_i(0)$. The error transformation function is introduced to realize the finite-time performance control scheme.

If a function $\rho_i(\varepsilon_i(t))$ has the following characters: The variable $\rho_i(\varepsilon_i(t))$ is a smooth and strictly increasing function with $-1 < \rho_i(\varepsilon_i(t)) < 1$. And, one has $\lim_{\varepsilon_i(t) \to +\infty} \rho_i(\varepsilon_i(t)) = 1$ and $\lim_{\varepsilon_i(t) \to -\infty} \rho_i(\varepsilon_i(t)) = -1$, where ε_i means a transformed error and the error $z_{i,1}(t)$ is related to $\varepsilon_i(t)$ by

$$z_{i,1}(t) = \zeta_i(t)\rho_i(\varepsilon_i(t)). \tag{16}$$

The tracking error $z_{i,1}(t)$ will be confined in the set $\Omega = \left\{z_{i,1}(t) \in R : \left|z_{i,1}(t)\right| \leq \zeta_i(T_0), t \geq T_0\right\}$, which is the mathematical explanation of the FTPF method.

Then, the error transformation function is selected as follows:

$$\rho_i(\varepsilon_i(t)) = \frac{2}{\pi} \arctan(\varepsilon_i(t)). \tag{17}$$

Because of the consideration of the communication time delays, the novel model will be given by considering the following change of coordinate. Consider the following local neighborhood synchronization errors as

$$z_{i,1} = \sum_{\pi=1}^{N} a_{i,\pi}\left(y_i - y_\pi(t - \tau_{i,\pi}(t))\right) + b_i(y_i - y_r), \tag{18}$$

where b_i is the pinning gain with $b_i \geq 0$. Since this paper considers the problem of time-delay in channels for information transmission between agents, the neighbor agents with time-delay phenomenon is shown as $y_\pi(t - \tau_{i,\pi}(t))$.

Differentiating (16) with respect to time yields

$$\dot{z}_{i,1} = \dot{\zeta}_i(t)\rho_i(\varepsilon_i(t)) + \zeta_i(t)\frac{\partial \rho_i(\varepsilon_i(t))}{\partial \varepsilon_i(t)}\dot{\varepsilon}_i(t). \tag{19}$$

Then, we can get

$$\dot{\varepsilon}_i(t) = \Theta_i(\varepsilon_i(t), \zeta_i(t)) + \psi_i(\varepsilon_i(t), \zeta_i(t))\dot{z}_{i,1}(t), \tag{20}$$

where

$$\Theta_i(\varepsilon_i(t),\zeta_i(t)) = -\frac{\dot{\zeta}_i(t)\rho_i(\varepsilon_i(t))}{\zeta_i(t)\frac{\partial\rho_i(\varepsilon_i(t))}{\partial\varepsilon_i(t)}} \tag{21}$$

and

$$\psi_i(\varepsilon_i(t),\zeta_i(t)) = \frac{1}{\zeta_i(t)\frac{\partial\rho_i(\varepsilon_i(t))}{\partial\varepsilon_i(t)}}. \tag{22}$$

2.6 Input Quantification

The system input $Q_i(u_i)$ is the quantized value of the control signal u_i, and the following hysteretic quantizer is used [36]

$$Q_i(u_i)=\begin{cases} u_{i,\varsigma}\mathrm{sgn}(u_i), & \frac{u_{i,\varsigma}}{1+\epsilon_i} < |u_i| \le u_{i,\varsigma}, \dot{u}_i<0, \text{ or} \\ & u_{i,\varsigma} < |u_i| \le \frac{u_{i,\varsigma}}{1-\epsilon_i}, \dot{u}_i>0. \\ u_{i,\varsigma}(1+\epsilon_i)\mathrm{sgn}(u_i), & u_{i,\varsigma} < |u_i| \le \frac{u_{i,\varsigma}}{1-\epsilon_i}, \dot{u}_i>0, \text{ or} \\ & \frac{u_{i,\varsigma}}{1-\epsilon_i} < |u_i| \le \frac{u_{i,\varsigma}(1+\epsilon_i)}{1-\epsilon_i}\dot{u}_i>0. \\ 0, & 0 \le |u_i| < \frac{u_{i,\min}}{1+\epsilon_i}, \dot{u}_i>0, \text{ or} \\ & \frac{u_{i,\min}}{1+\epsilon_i} \le |u_i| \le u_{i,\min}, \dot{u}_i>0. \\ Q_i(u_i(t^-)), & \text{othercases}, \end{cases} \tag{23}$$

where $u_{i,\varsigma} = q_i^{1-\varsigma}u_{i,\min}$ and $\bar{u}_{i,\varsigma} = u_{i,\varsigma}(1+\epsilon_i)$. The size of the dead-zone of the quantizer is denoted as $u_{i,min}$. The parameters q_i, ς and ϵ_i need to be satisfied with $0<q_i<1$, $\varsigma = 1,2,\ldots,u_{i,\min}>0$ and $\epsilon_i = \frac{1-q_i}{1+q_i}$. The variable $Q_i(u_i)$ exists in the set $U_i = \{0, \pm u_{i,\varsigma}, \pm u_{i,\varsigma}\}$. The status prior to $Q_i(u_i)$ is indicated as $Q_i(u_i(t^-))$.

3 Controller Design

Using the backstepping technique, a novel communication channels time-delay classification-based method for MASs is proposed with modified switching ET strategy.

The change of coordinates is used as

$$\begin{aligned} z_{i,1} &= \varepsilon_{i,1} \\ z_{i,\iota} &= x_{i,\iota} - \alpha_{i,\iota-1}, \end{aligned} \tag{24}$$

where $\alpha_{i,\iota-1}$ means the virtual controller.

The situation of large time-delay is discussed when $\tau_{i,r} = \tau_{i,r,\max}$ due to the large impact on system performance and determine it through the designed classification method.

The FTPF is used to obtain the predefined accuracy, one gets

$$\begin{aligned} \dot{\varepsilon}_{i,1}(t) &= \Theta_i(\varepsilon_i(t),\zeta_i(t)) + \psi_i(\varepsilon_i(t),\zeta_i(t)) \times \dot{z}_{i,1}(t) \\ &= \psi_i(\psi_i^{-1}\Theta_i + \dot{z}_{i,1}) \\ &= \psi_i(\psi_i^{-1}\Theta_i + \dot{\varepsilon}_{i,1}). \end{aligned}$$

Then, one has

$$\begin{aligned} \dot{\varepsilon}_{i,1}(t) = \psi_i\big(&\psi_i^{-1}\Theta_i + (d_i+b_i)(x_{i,2}+F_{i,1}+\varpi_{i,1}) \\ &- d_i(x_{\pi,2}+F_{\pi,1}+q_{\pi,1}(x_{\pi,1}(t-\tau_{i,\pi}(t))) \\ &+ \varpi_{\pi,1}) - b_i\dot{y}_r\big) \\ = \psi_i\big(&(b_i+d_i)x_{i,2} + K_{i,1} - d_i q_{\pi,1}(x_{\pi,1}(t-\tau_{i,\pi}(t)))\big) \end{aligned}$$

where

$$\begin{aligned} K_{i,1} = {}& \psi_i^{-1}\Theta_i + (b_i+d_i)F_{i,1} + (b_i+d_i)\varpi_{i,1} + d_i F_{\pi,1} \\ & - d_i x_{\pi,2} + d_i\varpi_{\pi,1} - b_i\dot{y}_r. \end{aligned}$$

Step 1: Pick the Lyapunov function candidate as

$$\begin{aligned} V_{i,1} = {}& \frac{1}{2\psi_i}\varepsilon_{i,1}^2 + \int_{t-\tau_{i,\pi}}^{t}\frac{1}{\psi_i}\varepsilon_{\pi,1}^2(\tau_{i,\pi})q_{\pi,1}^2(\bar{\varepsilon}_{i,1}(\tau_{i,\pi}))d\tau_{i,\pi} \\ & + \frac{1}{2}\tilde{\omega}_{i,1}^T\tilde{\omega}_{i,1} \end{aligned} \tag{25}$$

where $\tilde{\omega}_{i,1}$ means the approximation error.

The derivative of Eq. 25 is calculated as

$$\begin{aligned} \dot{V}_{i,1} = {}& \frac{1}{\psi_i}\big(\varepsilon_{i,1}^2 q_{\pi,1}^2(\bar{\varepsilon}_{i,1}) - \varepsilon_{i,1}^2(t-\tau_{i,\pi})q_{\pi,1}^2(\bar{\varepsilon}_{i,1}(t-\tau_{i,\pi}))\big) \\ & - \tilde{\omega}_{i,1}^T\dot{\hat{\omega}}_{i,1} + \frac{1}{4\psi_i^2}(4\varepsilon_{i,1}\dot{\varepsilon}_{i,1} - 2\varepsilon_{i,1}^2\dot{\psi}_i) \\ = {}& \frac{1}{\psi_i}\big(\varepsilon_{i,1}^2 q_{\pi,1}^2(\bar{\varepsilon}_{i,1}) - \varepsilon_{i,1}^2(t-\tau_{i,\pi})q_{\pi,1}^2(\bar{\varepsilon}_{i,1}(t-\tau_{i,\pi}))\big) \\ & - \tilde{\omega}_{i,1}^T\dot{\hat{\omega}}_{i,1} - \frac{\varepsilon_{i,1}\dot{\varepsilon}_{i,1}}{\psi_i} - \frac{\varepsilon_{i,1}^2\dot{\psi}_i}{2\psi_i^2} \\ = {}& \frac{1}{\psi_i}\big(\varepsilon_{i,1}^2 q_{\pi,1}^2(\bar{\varepsilon}_{i,1}) - \varepsilon_{i,1}^2(t-\tau_{i,\pi})q_{\pi,1}^2(\bar{\varepsilon}_{i,1}(t-\tau_{i,\pi}))\big) \\ & - \tilde{\omega}_{i,1}^T\dot{\hat{\omega}}_{i,1} - \frac{1}{2\psi_i}(b_i+d_i)(z_{i,2}+\alpha_{i,1})\varepsilon_{i,1}^2 - \frac{K_{i,1}\varepsilon_{i,1}^2}{2\psi_i} \\ & + \frac{1}{2\psi_i}d_i\varepsilon_{i,1}^2 q_{\pi,1}(x_{\pi,1}(t-\tau_{i,\pi})). \end{aligned}$$

With the aid of the Young's inequality, one has

$$\begin{aligned} & \frac{1}{2\psi_i}d_i\varepsilon_{i,1}^2 q_{\pi,1}(x_{\pi,1}(t-\tau_{i,\pi})) \\ \le {}& \frac{1}{16\psi_i}d_i^2\varepsilon_{i,1}^4 + \frac{1}{\psi_i}\varepsilon_{i,1}^2(t-\tau_{i,\pi})q_{\pi,1}^2(\bar{\varepsilon}_{\pi,1}(t-\tau_{i,\pi})). \end{aligned} \tag{26}$$

Then, one gets

$$\dot{V}_{i,1} \le \frac{1}{\psi_i}\varepsilon_{i,1}^2 q_{\pi,1}^2(\bar{\varepsilon}_{i,1}) - \frac{1}{2\psi_i}(b_i+d_i)(z_{i,2}+\alpha_{i,1})\varepsilon_{i,1}^2$$

$$+\frac{1}{16\psi_i}d_i^2\varepsilon_{i,1}^4-\tilde{\omega}_{i,1}^T\dot{\hat{\omega}}_{i,1}-\frac{1}{2\psi_i}(b_i+d_i)c_{i,1}'\varepsilon_{i,1}^3$$
$$+\frac{1}{2\psi_i}(b_i+d_i)c_{i,1}'\varepsilon_{i,1}^3-\frac{K_{i,1}\varepsilon_{i,1}^2}{2\psi_i}$$
$$+\frac{1}{2\psi_i}d_i\varepsilon_{i,1}^2q_{\pi,1}(x_{\pi,1}(t-\tau_{i,\pi})) \tag{27}$$

where $c_{i,1}'$ is a positive constant.

Then, one has

$$F_{i,1}=K_{i,1}-d_iq_{\pi,1}(x_{\pi,1}(t-\tau_{i,\pi}))+\frac{1}{2\psi_i}(b_i+d_i)c_{i,1}'\varepsilon_{i,1}^3$$
$$=\omega_{i,1}^T\delta_{i,1}+\upsilon_{i,1}.$$

The virtual controller is constructed as

$$\alpha_{i,1}=\frac{2}{b_i+d_i}q_{\pi,1}^2-\frac{1}{b_i+d_i}\hat{\omega}_{i,1}+\frac{1}{8(b_i+d_i)}d_i^2\varepsilon_{i,1}^2$$
$$+\frac{2}{b_i+d_i}c_{i,1}-c_{i,1}'\varepsilon_{i,1} \tag{28}$$

where $c_{i,1}$ is a designed parameter. The variable $\hat{\omega}_{i,1}$ is the estimated value of $\omega_{i,1}$ with $\tilde{\omega}_{i,1}=\omega_{i,1}-\hat{\omega}_{i,1}$.

The adaptive law is selected as

$$\dot{\hat{\omega}}_{i,1}=-\frac{1}{2\psi_i}(b_i+d_i)\varepsilon_{i,1}^2\delta_{i,1}-N_{i,1}\hat{\omega}_{i,1} \tag{29}$$

where $N_{i,1}$ is a constant with $N_{i,1}>0$.

Substituting (28) and (29) into (27), one has

$$\dot{V}_{i,1}\le-\frac{1}{\psi_i}(b_i+d_i)\varepsilon_{i,1}^2z_{i,2}-\frac{1}{\psi_i}c_{i,1}\varepsilon_{i,1}^2-\frac{N_{i,1}}{2}\tilde{\omega}_{i,1}^2$$
$$+\frac{N_{i,1}}{2}\omega_{i,1}^2+\frac{1}{2}\upsilon_{i,1}^2. \tag{30}$$

Step ι($\iota=2,\ldots,n-1$): The derivative of the virtual signal can be estimated by the SSMIF, one gets

$$\dot{\alpha}_{i,\iota-1}=R_{i,\iota 20}-R_{i,r_{\iota-1}}. \tag{31}$$

Pick the Lyapunov function candidate $V_{i,\iota}$ as

$$V_{i,\iota}=V_{i,\iota-1}+\frac{1}{2}z_{i,\iota}^2+\frac{1}{2}\tilde{\omega}_{i,\iota}^T\tilde{\omega}_{i,\iota} \tag{32}$$

where $\tilde{\omega}_{i,\iota}$ means the approximation error.

The derivative of Eq. 32 is calculated as

$$\dot{V}_{i,\iota}=\dot{V}_{i,\iota-1}+z_{i,\iota}\dot{z}_{i,\iota}-\tilde{\omega}_{i,\iota}^T\dot{\hat{\omega}}_{i,\iota}$$
$$=\dot{V}_{i,\iota-1}+z_{i,\iota}(x_{i,\iota+1}+F_{i,\iota}(\bar{x}_{i,\iota})+\varpi_{i,\iota}-\dot{\alpha}_{i,\iota-1})$$
$$-\tilde{\omega}_{i,\iota}^T\dot{\hat{\omega}}_{i,\iota}$$
$$=\dot{V}_{i,\iota-1}+z_{i,\iota}(z_{i,\iota+1}+\alpha_{i,\iota}+F_{i,\iota}+\varpi_{i,\iota}$$
$$-R_{i,\iota 20}+R_{i,r_{\iota-1}})-\tilde{\omega}_{i,\iota}^T\dot{\hat{\omega}}_{i,\iota}. \tag{33}$$

Under the explanation of Lemma 3, FLSs are often used to approximate unknown nonlinear terms. With the aid of the FLSs, one gets

$$F_{i,\iota}=\omega_{i,\iota}^T\delta_{i,\iota}+\upsilon_{i,\iota}.$$

Based on the Young's inequality, one has

$$z_{i,\iota}\upsilon_{i,\iota}\le\frac{1}{2}z_{i,\iota}^2+\frac{1}{2}\upsilon_{i,\iota}^2$$
$$z_{i,\iota}R_{i,r_{\iota-1}}\le\frac{1}{2}z_{i,\iota}^2+\frac{1}{2}R_{i,r_{\iota-1}}^2.$$

The virtual controller is designed as

$$\alpha_{i,\iota}=-c_{i,\iota}z_{i,\iota}-\hat{\omega}_{i,\iota}\delta_{i,\iota}+R_{i,\iota 20}-2z_{i,\iota}-z_{i,\iota-1} \tag{34}$$

where $c_{i,\iota}$ is a designed constant. The variable $\hat{\omega}_{i,\iota}$ is the estimated value of $\omega_{i,\iota}$ with $\tilde{\omega}_{i,\iota}=\omega_{i,\iota}-\hat{\omega}_{i,\iota}$.

The adaptive law is selected as

$$\dot{\hat{\omega}}_{i,\iota}=z_{i,\iota}\delta_{i,\iota}-N_{i,\iota}\hat{\omega}_{i,\iota} \tag{35}$$

where $N_{i,\iota}$ is a designed constant.

Substituting (34) and (35) into (33), it follows that

$$\dot{V}_{i,\iota}\le-\frac{1}{\psi_i}c_{i,1}\varepsilon_{i,1}^2-c_{i,\iota}z_{i,\iota}^2-\sum_{\varsigma=2}^{\iota}c_{i,\varsigma}z_{i,\varsigma}^2+\sum_{\varsigma=2}^{\iota}\frac{1}{2}\upsilon_{i,\varsigma}^2$$
$$+\sum_{\varsigma=2}^{\iota}\frac{1}{2}R_{i,r_{\varsigma-1}}^2-\sum_{\varsigma=2}^{\iota}\frac{N_{i,\varsigma}}{2}\tilde{\omega}_{i,\varsigma}^2+\sum_{\varsigma=2}^{\iota}\frac{N_{i,\varsigma}}{2}\omega_{i,\varsigma}^2$$
$$+\sum_{\varsigma=2}^{\iota}\frac{1}{2}\varpi_{i,\varsigma}^{*2}.$$

Step n: For the step n, the SSMIF is designed, and one has

$$\dot{\alpha}_{i,n-1}=R_{i,n20}-R_{i,r_{n-1}}. \tag{36}$$

Set the Lyapunov function candidate $V_{i,n}$ as

$$V_{i,n}=V_{i,n-1}+\frac{1}{2}z_{i,n}^2+\frac{1}{2}\tilde{\omega}_{i,n}^T\tilde{\omega}_{i,n} \tag{37}$$

where $\tilde{\omega}_{i,n}$ means the approximation error.

The derivation of Eq. 37 is expressed as

$$\dot{V}_{i,n}=\dot{V}_{i,n-1}+z_{i,n}(D_i(u_i)+P_i(t)+F_{i,n}+\varpi_{i,n}-R_{i,n20}$$
$$+R_{i,r_{n-1}})-\tilde{\omega}_{i,n}^T\dot{\hat{\omega}}_{i,n}. \tag{38}$$

Taking advantage of the Young's inequality, one obtains

$$z_{i,n}P_i(t)\le\frac{1}{2}z_{i,n}^2+\frac{1}{2}u_{i,\min}^2. \tag{39}$$

Substituting (38) and (39), it follows that

$$\begin{aligned}\dot{V}_{i,n} \leq & -\frac{1}{\psi_i}c_{i,1}\varepsilon_{i,1}^2-\sum_{\varphi=2}^{n-1}c_{i,\varphi}z_{i,\varphi}^2+\sum_{\varphi=2}^{n-1}\frac{1}{2}\upsilon_{i,\varphi}^2+\sum_{\varphi=2}^{n-1}\frac{1}{2}R_{i,r_{\varphi-1}}^2\\ & -\sum_{\varphi=2}^{n-1}\frac{N_{i,\varphi}}{2}\tilde{\omega}_{i,\varphi}^2+\sum_{\varphi=2}^{n-1}\frac{N_{i,\varphi}}{2}\omega_{i,\varphi}^2+\sum_{\varphi=2}^{n-1}\frac{1}{2}\varpi_{i,\varphi}^{*2}\\ & +z_{i,n}(D_i(u_i)+P_i(t)+F_{i,n}+\varpi_{i,n}-R_{i,n20}\\ & +R_{i,r_{n-1}})-\tilde{\omega}_{i,n}^T\dot{\hat{\omega}}_{i,n}.\end{aligned}$$

With the aid of the FLSs, one obtains

$$F_{i,\iota}=\omega_{i,\iota}^T\delta_{i,\iota}+\upsilon_{i,\iota}. \tag{40}$$

According to the the Young's inequality, one has

$$\begin{aligned}z_{i,n}\upsilon_{i,n} &\leq \frac{1}{2}z_{i,n}^2+\frac{1}{2}\upsilon_{i,n}^2\\ z_{i,n}R_{i,r_{n-1}} &\leq \frac{1}{2}z_{i,n}^2+\frac{1}{2}R_{i,r_{n-1}}^2.\end{aligned}$$

The modified switching ET strategy is proposed as

$$t_{i,\Gamma+1}=\begin{cases}\inf\left\{t\in R \mid \left|E_i(t)\right| \geq \varrho_i\left|u_i(t)\right|+l_{i,1}\right\} & \left|z_{i,n}\right|<\phi_i\\ \inf\left\{t\in R \mid \left|E_i(t)\right| \geq l_{i,2}\right\} & \left|z_{i,n}\right|\geq\phi_i.\end{cases} \tag{41}$$

Based on the modified switching ET strategy, there is $\mu_{i,1}(t)\in[0,1]$ and $\mu_{i,2}(t)\in[0,1]$, and the following equations hold

$$u_i(t)=\frac{\vartheta_i(t)}{1+\mu_{i,1}(t)\varrho_i}-\frac{\mu_{i,2}(t)l_{i,1}}{1+\mu_{i,1}(t)\varrho_i} \tag{42}$$

$$\vartheta_i(t)=-(1+\varrho_i)\left(\alpha_{i,n}\tanh\left(\frac{\alpha_{i,n}z_{i,n}}{\Psi_i}\right)+\bar{l}_{i,1}\tanh\left(\frac{\bar{l}_{i,1}z_{i,n}}{\Psi_i}\right)\right) \tag{43}$$

where $\bar{l}_{i,1}$ is a variable with $\bar{l}_{i,1}>\frac{l_{i,1}}{1-\varrho_i}$.

The controller and the adaptive law are constructed as

$$\alpha_{i,n}=\frac{1}{1-\gamma_i}(-c_{i,n}z_{i,n}-\hat{\omega}_{i,n}\delta_{i,n}+R_{i,n20}-\frac{5}{2}z_{i,n}-z_{i,n-1}) \tag{44}$$

and

$$\dot{\hat{\omega}}_{i,n}=z_{i,n}\delta_{i,n}-N_{i,n}\hat{\omega}_{i,n} \tag{45}$$

where Ψ_i, $N_{i,n}$ and $c_{i,n}$ are positive constants. The variable $\hat{\omega}_{i,n}$ is the estimated value of $\omega_{i,n}$ with $\tilde{\omega}_{i,n}=\omega_{i,n}-\hat{\omega}_{i,n}$.

Then, it follows that

$$\begin{aligned}\dot{V}_{i,n} \leq & -\frac{1}{\psi_i}c_{i,1}\varepsilon_{i,1}^2-\sum_{\eta=2}^{n}c_{i,\eta}z_{i,\eta}^2+\sum_{\eta=2}^{n}\frac{1}{2}\upsilon_{i,\eta}^2+\sum_{\eta=2}^{n}\frac{1}{2}R_{i,r_{\eta-1}}^2\\ & +0.557\kappa_i-\sum_{\eta=2}^{n}\frac{N_{i,\eta}}{2}\tilde{\omega}_{i,\eta}^2+\sum_{\eta=2}^{n}\frac{N_{i,\eta}}{2}\omega_{i,\eta}^2+\sum_{\eta=2}^{n}\frac{1}{2}\varpi_{i,\eta}^{*2}\\ & -\left|z_{i,n}\bar{l}_{i,1}\right|+\left|\frac{z_{i,n}l_{i,1}}{1-\varrho_i}\right|.\end{aligned}$$

Based on this, one obtains

$$\begin{aligned}\dot{V}_{i,n} \leq & -\frac{1}{\psi_i}c_{i,1}\varepsilon_{i,1}^2-\sum_{\eta=2}^{n}c_{i,\eta}z_{i,\eta}^2+\sum_{\eta=2}^{n}\frac{1}{2}\upsilon_{i,\eta}^2+\sum_{\eta=2}^{n}\frac{1}{2}R_{i,r_{\eta-1}}^2\\ & -\sum_{\eta=2}^{n}\frac{N_{i,\eta}}{2}\tilde{\omega}_{i,\eta}^2+\sum_{\eta=2}^{n}\frac{N_{i,\eta}}{2}\omega_{i,\eta}^2+\sum_{\eta=2}^{n}\frac{1}{2}\varpi_{i,\eta}^{*2}+0.557\kappa_i.\end{aligned}$$

Remark 3 The FTPF is considered to design the adaptive controller for the MASs with communication time-delay and input quantification. The proposed scheme in this paper is more universal than the results which can only solve this problem in the single-input single-output system.

4 Stability Analysis

Theorem 1 *Consider the MASs* (1) *subject to input quantization* (23) *and communication time-delay under* Assumptions 1 and 2. *The adaptive laws* (29), (35) *and* (45), *ET adaptive controller* (41), *and the distributed controllers* (28), (34) *and* (44) *ensure that all the closed-loop signals keep bounded. For* $\forall\lambda>0$, *the design parameters are turned such that*

$$\lim_{t\to\infty}\|y-y_r\|\leq\lambda. \tag{46}$$

Proof The stability of the overall closed-loop system is analysed, and we choose the total Lyapunov candidate function V as

$$V=\sum_{i=1}^{N}V_{i,n}. \tag{47}$$

The derivative of Eq. 47 satisfies

$$\dot{V}=\sum_{i=1}^{N}\dot{V}_{i,n}. \tag{48}$$

Then, one has

$$\dot{V} \leq -\sum_{i=1}^{N}\frac{1}{\psi_i}c_{i,1}\varepsilon_{i,1}^2 - \sum_{i=2}^{N}\sum_{\eta=2}^{n}c_{i,\eta}z_{i,\eta}^2 + \sum_{i=1}^{N}\sum_{\eta=1}^{n}\frac{1}{2}\upsilon_{i,\eta}^2 + \sum_{i=1}^{N}\sum_{\eta=2}^{n}\frac{1}{2}R_{i,r_{\eta-1}}^2 - \sum_{i=1}^{N}\sum_{\eta=1}^{n}\frac{N_{i,\eta}}{2}\tilde{\omega}_{i,\eta}^2 + \sum_{i=1}^{N}\sum_{\eta=1}^{n}\frac{N_{i,\eta}}{2}\omega_{i,\eta}^2 + \sum_{i=1}^{N}\sum_{\eta=2}^{n}\frac{1}{2}\varpi_{i,\eta}^{*2} + \sum_{i=1}^{N}0.557\kappa_i.$$

Using the above-mentioned analysis, the result is rewritten as

$$\dot{V} \leq -CV + D, \tag{49}$$

where

$$C = \min\left\{c_{i,1}, c_{i,\eta}, N_{i,\eta}\right\} \tag{50}$$

and

$$D = \sum_{i=1}^{N}\sum_{\eta=1}^{n}\frac{N_{i,\eta}}{2}\omega_{i,\eta}^2 + \sum_{i=1}^{N}\sum_{\eta=2}^{n}\frac{1}{2}\varpi_{i,\eta}^{*2} + \sum_{i=1}^{N}0.557\kappa_i + \sum_{i=1}^{N}\sum_{\eta=1}^{n}\frac{1}{2}\upsilon_{i,\eta}^2 + \sum_{i=1}^{N}\sum_{\eta=2}^{n}\frac{1}{2}R_{i,r_{\eta-1}}^2.$$

Multiplying both sides by e^{Ct} and integrating both sides it over $[0, t]$, one has

$$0 \leq V(t) \leq e^{-Ct}V(0) + \frac{D}{C}(1 - e^{-Ct}). \tag{51}$$

According to the definition of V and Eq. 51, we can get

$$|| s_{.1} ||^2 \leq 2e^{-Ct}V(0) + \frac{2D}{C}(1 - e^{-Ct}). \tag{52}$$

From the definition of C and D, for $\forall H > 0$, by choosing proper parameters, we have

$$\frac{D}{C} \leq \frac{H^2}{2}(\sigma(\mathcal{L} + \mathcal{B}))^2. \tag{53}$$

When $t \to \infty$, according to Lemma 2, the inequality (46) holds, and all signals are SGUUB.

Next, the Zeno phenomenon under the modified switching ET mechanism will be excluded. Based on the equation $E_i(t) = \vartheta_i(t) - u_i(t)$, one has

$$\frac{d\left|E_i(t)\right|}{dt} = \dot{E}_i \text{sign}(\dot{E}_i) \leq \left|\dot{\vartheta}_i\right|. \tag{54}$$

Since ϑ_i means a function consisting of bounded variable, the upper bound of $\left|\dot{\vartheta}_i\right|$ is existing with $\left|\dot{\vartheta}_i\right| \leq \vartheta_i^*$. Hence, one gets

$$\left|E_i(t)\right| = \int_{t_{i,\Gamma}}^{t_{i,\Gamma+1}}\left|\dot{\vartheta}_i\right|dt \leq \int_{t_{i,\Gamma}}^{t_{i,\Gamma+1}}\vartheta_i^* dt \leq \vartheta_i^*(t_{i,\Gamma+1} - t_{i,\Gamma}). \tag{55}$$

The lower bound of $\left|E_i(t)\right|$ is got with $\left|E_i(t)\right| > \phi_i$.

Hence, the following inequality holds

$$t_{i,\Gamma+1} - t_{i,\Gamma} \geq \frac{\phi_i}{\vartheta_i^*} > 0. \tag{56}$$

Due to the lower bound of the proposed ET interval being positive, the Zeno behavior is eliminated.

5 Simulation Results

In this section, the effectiveness of the proposed control strategy is demonstrated by two simulation examples. A novel communication time-delay classification-based method is constructed for MASs with the FPPF. Through the designed control plan, the expected control objectives are achieved, and the control tasks are completed. Some simulation results presented herein verify the effectiveness of the proposed control methodology.

The topology of the communication is depicted in Fig. 1.

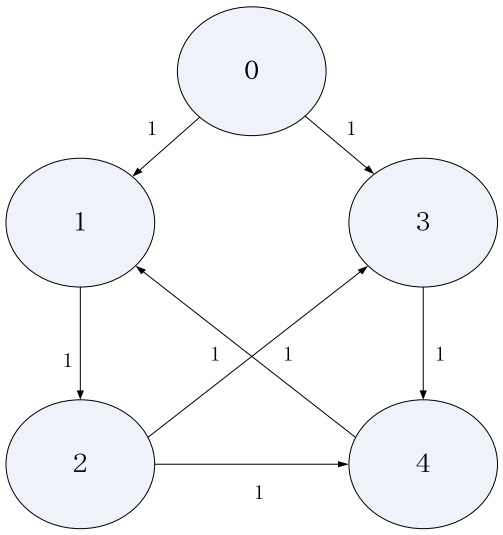

Fig. 1 The topology of the communication

Based on Fig. 1, the adjacency matrix $\mathcal{A}$ and the Laplacian matrix $\mathcal{L}$ are shown as follows:

$$\mathcal{A} = \begin{bmatrix} 0 & 0 & 0 & 1 \\ 1 & 0 & 0 & 0 \\ 0 & 1 & 0 & 0 \\ 0 & 1 & 1 & 0 \end{bmatrix}, \mathcal{L} = \begin{bmatrix} 1 & 0 & 0 & -1 \\ -1 & 1 & 0 & 0 \\ 0 & -1 & 1 & 0 \\ 0 & -1 & -1 & 2 \end{bmatrix}.$$

5.1 Numerical Example

Consider the MASs consisting of four agents and one leader with a communication digraph. The dynamics of agent i for $i = 1, 2, 3, 4$ are described as

$$\begin{cases} \dot{x}_{i,1} = x_{i,2} + F_{i,1}(\bar{x}_{i,1}) + \varpi_{i,1} \\ \dot{x}_{i,2} = Q_i(u_i) + F_{i,2}(\bar{x}_{i,2}) + \varpi_{i,2} \\ y_i = x_{i,1} \end{cases} \tag{57}$$

where

$$F_{i,1}(\bar{x}_{i,1}) = x_{i,1}^2 \sin(x_{i,1})$$
$$F_{i,2}(\bar{x}_{i,2}) = -\sin(x_{i,1}) \sin(x_{i,2})$$

and

$$\varpi_{i,1} = x_{i,1} \cos(t)$$
$$\varpi_{i,2} = x_{i,1} x_{i,2} \sin(x_{i,1}).$$

The dynamic model of the leader is

$$y_r = 4 \sin(1.5t). \tag{58}$$

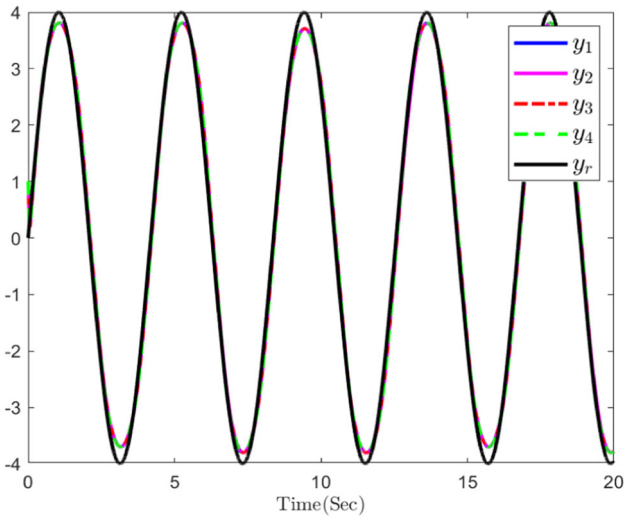

Fig. 2 The trajectories of four followers and the leader

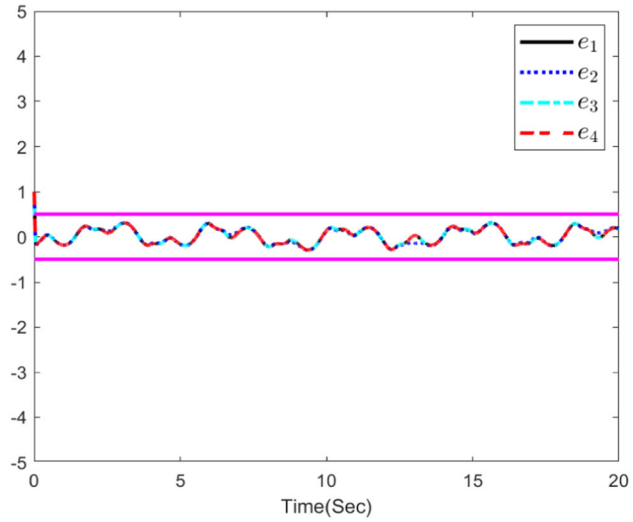

Fig. 3 The trajectories of tracking errors

Some associated simulation parameters are selected as $x_i(0) = [1, 0.1]^T$. Adaptive parameters are chosen to be $\hat{\omega}_{i,1}(0) = 0.1$ and $\hat{\omega}_{i,2}(0) = 0.1$. The parameters are chosen as $R_{i,210}(0) = R_{i,220}(0) = 0.1$, $c_{i,1} = c_{i,2} = 80$, $u_{i,\min} = 0.1$, $l_{i,1} = l_{i,2} = 0.1$, $\varrho_i = 0.1$, $\zeta_i(T_0) = 0.5$, $\zeta_{i,0} = 0.4$, $\nu_i = 1$, $k = 4$, $M = 0.05$, $\phi_i = 0.05$, $T_0 = 0.8$, $q_i = 0.1$, $\beta_i = 5$ and $N_{i,1} = N_{i,2} = 2$.

The curves of four followers and the leader are presented in Fig. 2, which demonstrates the rationality of the designed control scheme. The trajectories of tracking errors are certificated in Fig. 3. It follows from this figure that the considered method makes the tracking errors converge to a preset arbitrarily small region in the finite-time range. Figure 4 shows the trajectories of the input signals u_i, which proves the

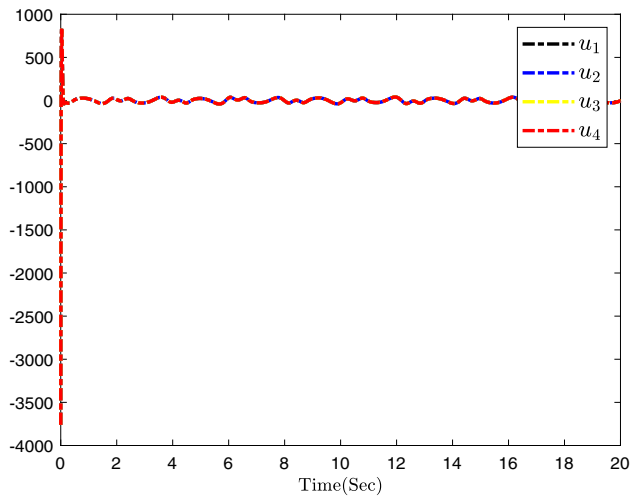

Fig. 4 The curves of controller input u_i

Fig. 5 The interevent times of agent i

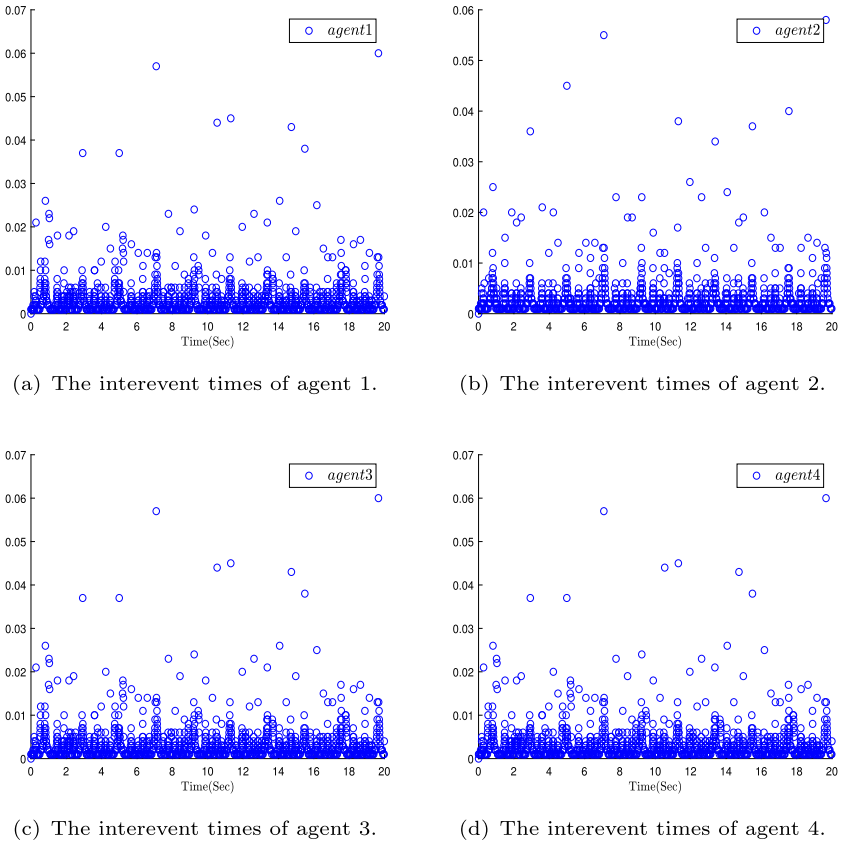

(a) The interevent times of agent 1.

(b) The interevent times of agent 2.

(c) The interevent times of agent 3.

(d) The interevent times of agent 4.

feasibility of considered control scheme. In Fig. 5, the triggering interval graph is used to show the time interval between adjacent moments of control updates. In the proposed ET mechanism, the fixed threshold ET mechanism is applied to flexibly adjust the number of updates when the error is larger than the designed switching value. It is observed that the update frequency will be higher because the system is in a relatively unstable state and more frequent updates are needed to make the system reach a stable state rapidly. Meanwhile, another case is illustrated when the error is smaller than the designed switching value and the system exists in a relatively more stable state. There is less need for frequent

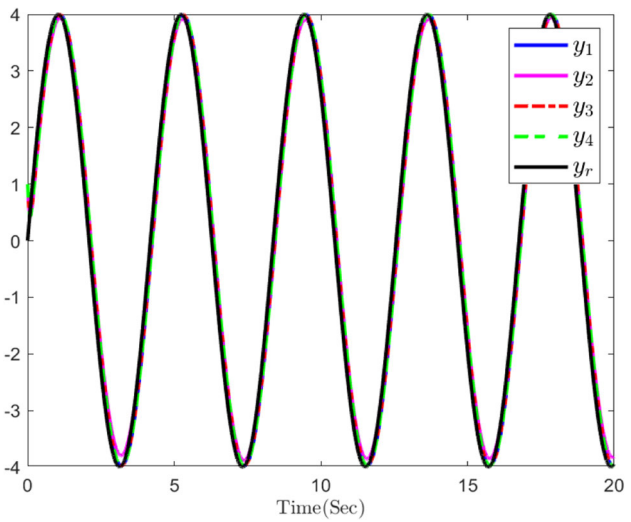

Fig. 6 The trajectories of the four followers and the leader

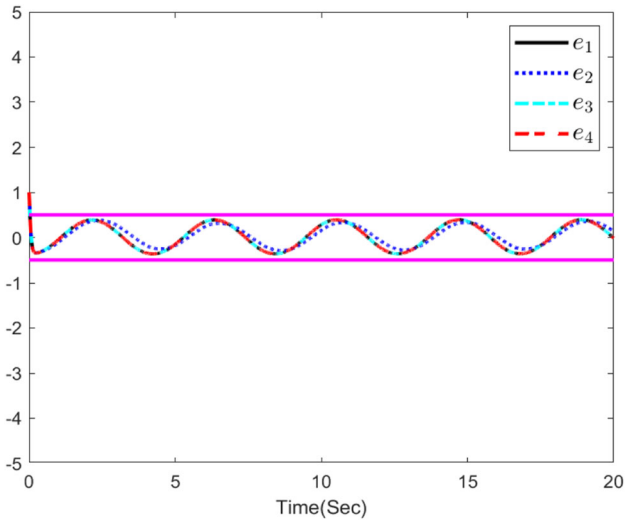

Fig. 7 The trajectories of tracking errors

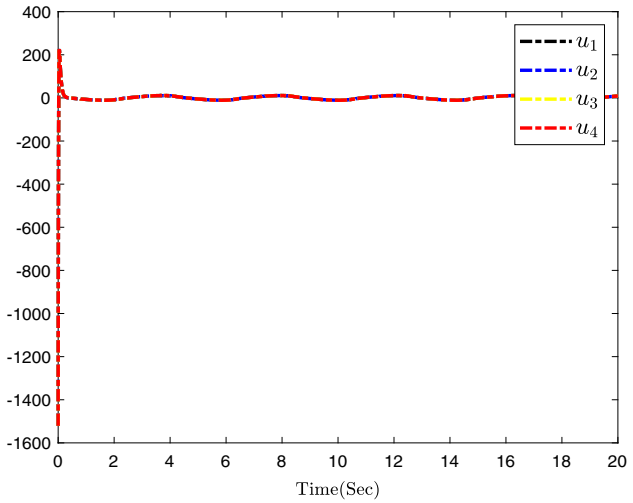

Fig. 8 The curves of controller input u_i

updates, when the relative threshold ET mechanism is used to achieve self-adjustment through the controller value to keep the controller reasonably updated, so that communication resources can be reasonably saved.

5.2 Practical Example

Choose a system of four multiple single-link robot manipulators depicted as

$$\lambda\ddot{h}_i + \Phi\dot{h}_i + \Upsilon \sin(h_i) + \bar{D}_s(h_i, \dot{h}_i) = \Xi_i \tag{59}$$

where some parameters are selected as $\lambda = 1$, $\Phi = 1$ and $\Upsilon = 10$, which the definition is found in [34] for details.

Defining $x_{i,1} = h_i$, $x_{i,2} = \dot{h}_i$, $\bar{D}_s(h_i, \dot{h}_i) = \varpi_{i,2}$ and $u_i = \Xi_i$, it follows that

$$\begin{cases} \dot{x}_{i,1} = x_{i,2} \\ \dot{x}_{i,2} = \dfrac{1}{\lambda} Q_i(u_i) + F_{i,2} + \varpi_{i,2} \end{cases} \tag{60}$$

where $F_{i,2} = -\frac{\Phi\dot{x}_{i,1} + \Upsilon \sin(x_{i,1})}{\lambda}$.

The communication topology and fuzzy membership functions adopted are identical to those used in the numerical example, while the initial states and linked parameters mirror those applied in the numerical simulation. Figure 6 is the tracking control result. It can be observed that the outputs y_i

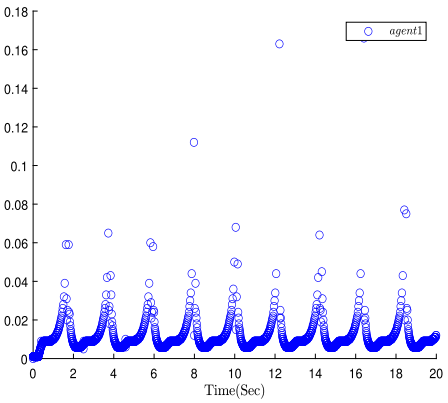

(a) The interevent times of agent 1.

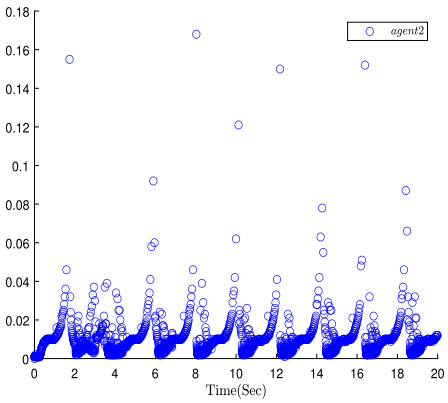

(b) The interevent times of agent 2.

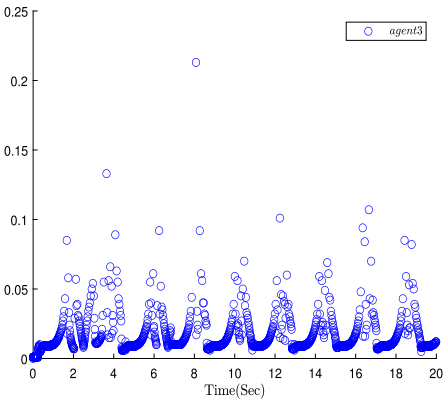

(c) The interevent times of agent 3.

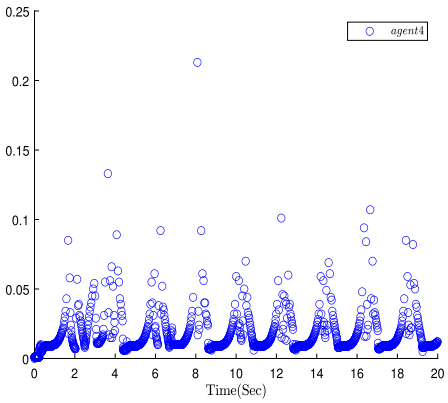

(d) The interevent times of agent 4.

Fig. 9 The interevent times of agent i for modified switching ET mechanism in this paper

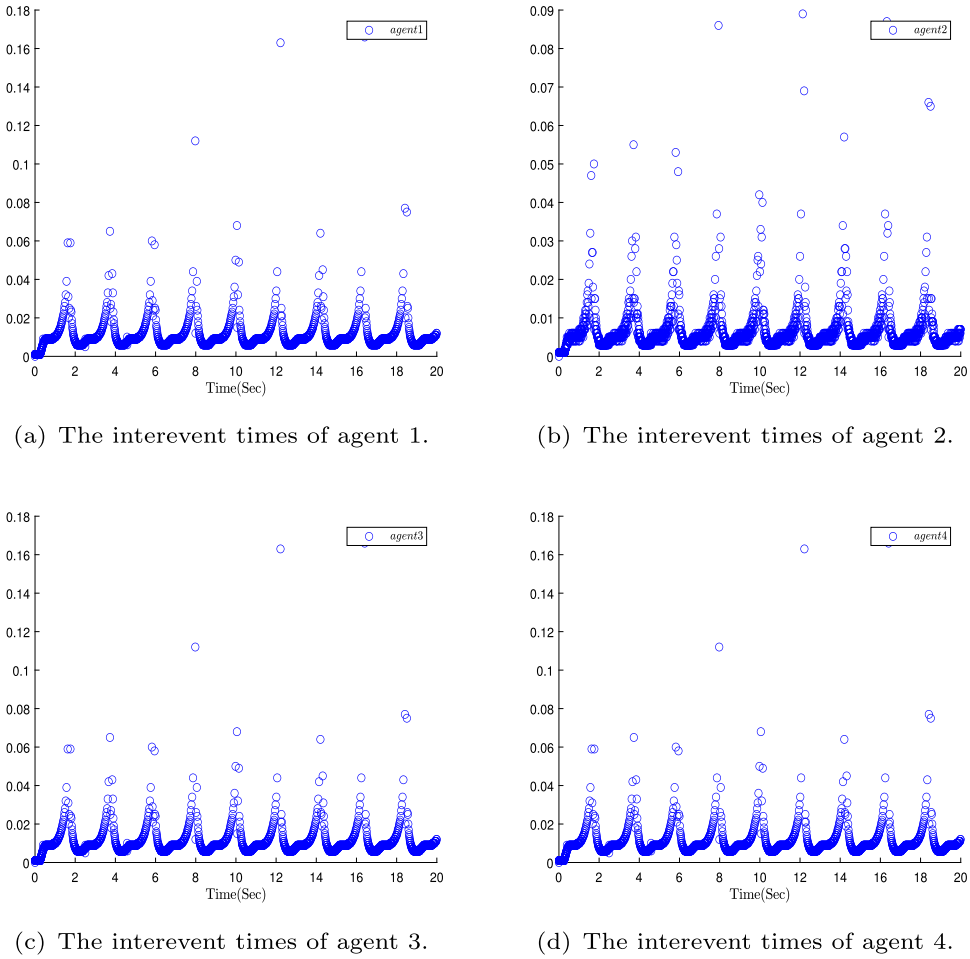

Fig. 10 The interevent times of agent i for switching ET mechanism in [31]

(a) The interevent times of agent 1.

(b) The interevent times of agent 2.

(c) The interevent times of agent 3.

(d) The interevent times of agent 4.

and the signal of leader y_r are consistent. In Fig. 7, this figure shows the trajectories of tracking errors, which converges to a preset arbitrarily small region in finite time range. Thus, it can indicate the usefulness of designed FTPF. The figure depicts the curves of input signals u_i, which means the proposed control strategy being effective in Fig. 8. In Fig. 9, the triggering interval graph is used to show the time interval between adjacent moments of control updates. When the tracking error becomes larger or smaller, the update frequency of the system can be appropriately increased or reduced. Figure 9 considers the switching ET mechanism based on synchronization error, while Fig. 10 considers the switching ET mechanism based on controller value. By comparing Figs. 9 and 10, it can be seen that the modified switching ET mechanism further saves communication resources while ensuring system tracking performance.

6 Conclusions

A novel communication time-delay classification-based method has been considered for nonlinear MASs with modified switching ET strategy. Firstly, a time-delay phenomenon for communication channels between agents has been investigated, which is solved by applying a unified Lyapunov-Krasovskii functional. Then, an improved time-delay classification method has been proposed to advance the accuracy of the classification mechanism by considering the degree of deviation and relative variation of neighbor agents. Moreover, a modified switching ET mechanism has been constructed to satisfy the need for reducing transmission burden, and it considers the impact of tracking errors on the threshold condition. Eventually, the suitability of suggested control method has been validated by two simulation examples. In the future, some new fields [37–43] will be investigated.

Acknowledgements This work was partially supported by the National Natural Science Foundation of China (62103108, 62303179), the General Cultivation of Scientific Research Projects of Bohai University (0522xn072), the Scientific Research Fund of Hunan Provincial Education Department (22B0468), the Science and Technology Project of Nantong City (MS22022060), the Revitalization of Liaoning Talents Program (XLYC2203201) and the Innovation Fund Project for Graduate Student of Bohai University (YJC2023-004).

Author Contributions All authors contributed to the study conception and design. Data simulation, manuscript revision and proofreading were

performed by Dongni Li, Liang Cao, Yingnan Pan, Wenbin Xiao and Hong Xue. The first draft of the manuscript was written by Dongni Li and all authors commented on previous versions of the manuscript. All authors read and approved the final manuscript.

Declarations

Ethics Approval The authors respect the Ethical Guidelines of the Journal.

Consent to Participate Informed consent was obtained from all individual participants included in the study.

Consent for Publication Not applicable.

Conflict of Interest The authors declare that they have no known competing financial interests or personal relationships that could have appeared to influence the work reported in this paper.

References

1. Chen, L., Liang, H., Pan, Y., Li, T.: Human-in-the-loop consensus tracking control for UAV systems via an improved prescribed performance approach. IEEE Trans. Aerospace Electronic Syst. (2023). https://doi.org/10.1109/TAES.2023.3304283
2. Pan, Y., Ji, W., Lam, H.-K., Cao, L.: An improved predefined-time adaptive neural control approach for nonlinear multiagent systems. IEEE Trans. Automation Sci. Eng. (2023). https://doi.org/10.1109/TASE.2023.3324397
3. Yang, S., Pan, Y., Cao, L., Chen, L.: Predefined-time fault-tolerant consensus tracking control for Multi-UAV systems with prescribed performance and attitude constraints. IEEE Trans. Aerospace Electronic Syst. (2024). https://doi.org/10.1109/TAES.2024.3371406
4. Qian, W., Lu, D., Guo, S.M., Zhao, Y.J.: Distributed state estimation for mixed delays system over sensor networks with multichannel random attacks and markov switching topology. IEEE Trans. Neural Netw. Learn. Syst. (2022). https://doi.org/10.1109/TNNLS.2022.3230978
5. Yao, D., Li, H., Shi, Y.: Event-based average consensus of disturbed MASs via fully distributed sliding mode control. IEEE Trans. Automatic Control (2023). https://doi.org/10.1109/TAC.2023.3317505
6. Yang, Y., Liu, Q., Yue, D., Han, Q.: Predictor-based neural dynamic surface control for bipartite tracking of a class of nonlinear multiagent systems. IEEE Trans. Neural Netw. Learn. Syst. **33**(4), 1791–1802 (2021)
7. Liu, Y., Chi, R., Wang, L., Lin, N.: HiTL-based adaptive fuzzy tracking control of mass: A distributed fixed-time strategy. Sci. China Technol. Sci. (2022). https://doi.org/10.1007/s11431-022-2319-6
8. Wang, M., Shi, H., Wang, C.: Distributed cooperative learning for discrete-time strict-feedback multi agent systems over directed graphs. IEEE/CAA J. Automatica Sinica **9**(10), 1831–1844 (2022)
9. Yaghoubi, Z., Talebi, H.A.: Cluster consensus for nonlinear multi-agent systems. J. Intell. Robotic Syst. **100**(3–4), 1069–1084 (2020)
10. Cao, L., Pan, Y., Liang, H., Huang, T.: Observer-based dynamic event-triggered control for multiagent systems with time-varying delay. IEEE Trans. Cybernetics **53**(5), 3376–3387 (2023)
11. Chen, Z.: Synchronization of frequency-modulated multiagent systems. IEEE Trans. Autom. Control **68**(6), 3425–3439 (2023)
12. Gao, H., An, H., Lin, W., Yu, X., Qiu, J.: Trajectory tracking of variable centroid objects based on fusion of vision and force perception. IEEE Trans. Cybernetics (2023). https://doi.org/10.1109/TCYB.2023.3240502
13. Yan, B., Niu, B., Zhao, X., Wang, H., Chen, W., Liu, X.: Neural-network-based adaptive event-triggered asymptotically consensus tracking control for nonlinear nonstrict-feedback MASs: An improved dynamic surface approach. IEEE Trans. Neural Netw. Learn. Syst. (2022). https://doi.org/10.1109/TNNLS.2022.3175956
14. Zhang, Y., Sun, J., Liang, H., Li, H.: Event-triggered adaptive tracking control for multiagent systems with unknown disturbances. IEEE Trans. Cybernetics **50**(3), 890–901 (2018)
15. Shang, Y., Chen, B., Lin, C.: Consensus tracking control for distributed nonlinear multiagent systems via adaptive neural backstepping approach. IEEE Trans. Syst. Man Cybernetics Syst. **50**(7), 2436–2444 (2018)
16. Lin, G., Li, H., Ma, H., Zhou, Q.: Distributed containment control for human-in-the-loop MASs with unknown time-varying parameters. IEEE Trans. Circuits Syst. I Regul. Pap. **69**(12), 5300–5311 (2022)
17. He, Y., Zhang, C.-K., Zeng, H.-B., Wu, M.: Additional functions of variable-augmented-based free-weighting matrices and application to systems with time-varying delay. Int. J. Syst. Sci. **54**(5), 991–1003 (2023)
18. Li, K., Ahn, C.K., Zheng, W., Hua, C.: A delay classification-based approach to distributed consensus of nonlinear time-delay multiagent systems. IEEE Trans. Autom. Control (2023). https://doi.org/10.1109/TAC.2023.3243536
19. Chen, K., Wang, J., Zhang, Y., Liu, Z.: Leader-following consensus for a class of nonlinear strick-feedback multiagent systems with state time-delays. IEEE Trans. Syst. Man Cybernetics Syst. **50**(7), 2351–2361 (2018)
20. Ma, J., Xu, S., Fei, S.: Asymptotic tracking control of nonlinear time-delay systems with mismatched disturbances. IEEE Trans. Circuits Syst. II Express Briefs **70**(1), 261–265 (2022)
21. Liu, Y., Liu, X., Jing, Y., Zhang, Z.: A novel finite-time adaptive fuzzy tracking control scheme for nonstrict feedback systems. IEEE Trans. Fuzzy Syst. **27**(4), 646–658 (2018)
22. Sui, S., Chen, C.P., Tong, S.: A novel full errors fixed-time control for constraint nonlinear systems. IEEE Trans. Autom. Control **68**(4), 2568–2575 (2023)
23. Li, Z., Park, J.H.: Dissipative fuzzy tracking control for nonlinear networked systems with quantization. IEEE Trans. Syst. Man Cybernetics Syst. **50**(12), 5130–5141 (2018)
24. Liang, H., Zhang, Y., Huang, T., Ma, H.: Prescribed performance cooperative control for multiagent systems with input quantization. IEEE Trans. Cybernetics **50**(5), 1810–1819 (2019)
25. Su, H., Cheng, B., Li, Z.: Cooperative output regulation of heterogeneous systems over directed graphs: A dynamic adaptive event-triggered strategy. J. Syst. Sci. Complexity **36**(3), 909–921 (2023)

26. Ren, H., Ma, H., Li, H., Wang, Z.: Adaptive fixed-time control of nonlinear MASs with actuator faults. IEEE/CAA J. Automatica Sinica **10**(5), 1252–1262 (2023)
27. Ren, H., Cheng, Z., Qin, J., Lu, R.: Deception attacks on event-triggered distributed consensus estimation for nonlinear systems. Automatica **154**, 111100 (2023)
28. Pan, Q., Li, Y., Ma, B., An, T., Zhou, F.: Event-triggered-based decentralized optimal control of modular robot manipulators using RNN identifier. J. Intell. Robotic Syst. **106**(3), 55 (2022)
29. Guo, X., Dong, Z., Wang, C., Ding, Z.: Event-based resilient distributed estimation under multiple heterogeneous cyberattacks. IEEE Trans. Control of Netw. Syst. **10**(2), 625–635 (2023)
30. Li, S., Ahn, C.K., Guo, J., Xiang, Z.: Neural-network approximation-based adaptive periodic event-triggered output-feedback control of switched nonlinear systems. IEEE Trans. Cybernetics **51**(8), 4011–4020 (2021)
31. Xing, L., Wen, C., Liu, Z., Su, H., Cai, J.: Event-triggered adaptive control for a class of uncertain nonlinear systems. IEEE Trans. Autom. Control **62**(4), 2071–2076 (2016)
32. Pang, N., Wang, X., Wang, Z.: Event-triggered adaptive control of nonlinear systems with dynamic uncertainties: the switching threshold case. IEEE Trans. Circuits Syst. II Express Briefs **69**(8), 3540–3544 (2022)
33. Wang, X., Zhou, Y., Huang, T., Chakrabarti, P.: Event-triggered adaptive fault-tolerant control for a class of nonlinear multiagent systems with sensor and actuator faults. IEEE Trans. Circuits Syst. I Regul. Pap. **69**(10), 4203–4214 (2022)
34. Wang, W., Liang, H., Pan, Y., Li, T.: Prescribed performance adaptive fuzzy containment control for nonlinear multiagent systems using disturbance observer. IEEE Trans. Cybernetics **50**(9), 3879–3891 (2020)
35. Jing, Y., Yang, G.: Fuzzy adaptive quantized fault-tolerant control of strict-feedback nonlinear systems with mismatched external disturbances. IEEE Trans. Syst. Man Cybernetics Syst. **50**(9), 3424–3434 (2018)
36. Xu, Y., Li, T., Yang, Y., Shan, Q., Tong, S., Chen, C.P.: Anti-attack event-triggered control for nonlinear multi-agent systems with input quantization. IEEE Trans. Neural Netw. Learn. Syst. (2022). https://doi.org/10.1109/TNNLS.2022.3164881
37. Tong, S., Sun, K., Sui, S.: Observer-based adaptive fuzzy decentralized optimal control design for strict-feedback nonlinear large-scale systems. IEEE Trans. Fuzzy Syst. **26**(2), 569–584 (2018)
38. Fu, J., Lv, Y., Yu, W.: Robust adaptive time-varying region tracking control of multi-robot systems. Sci. China Inf. Sci. **66**(5), 159202 (2023)
39. Gao, H., Li, Z., Yu, X., Qiu, J.: Hierarchical multi-objective heuristic for PCB assembly optimization in a beam-head surface mounter. IEEE Trans. Cybernetics **52**(7), 6911–6924 (2022)
40. Ma, Z., Ma, H.: Adaptive fuzzy backstepping dynamic surface control of strict-feedback fractional-order uncertain nonlinear systems. IEEE Trans. Fuzzy Syst. **28**(1), 122–133 (2019)
41. Guo, X., Wang, C., Dong, Z., Ding, Z.: Secure state estimation for nonlinear systems under sparse attacks with application to robotic manipulators. IEEE Trans. Industr. Electron. **70**(8), 8408–8415 (2023)
42. Hou, M., Shi, W., Fang, L., Duan, G.: Adaptive dynamic surface control of high-order strict feedback nonlinear systems with parameter estimations. Sci. China Inf. Sci. **66**(5), 159203 (2023)
43. Zhang, H., Zhao, X., Wang, H., Niu, B., Xu, N.: Adaptive tracking control for output-constrained switched MIMO pure-feedback nonlinear systems with input saturation. J. Syst. Sci. Complexity **36**(3), 960–984 (2023)

Dongni Li received the B.S. degree in automation from Bohai University, Jinzhou, China, in 2021, where she is currently pursuing the M.S. degree in control theory and control engineering. Her current research interests include cooperative control, adaptive fuzzy/neural control, and event-triggered control.

Liang Cao received the Ph.D. degree in control science and engineering from the Guangdong University of Technology, Guangzhou, China, in 2019. He was a Postdoctoral Researcher with the School of Automation, Guangdong University of Technology from 2020 to 2022. He is currently an Associate Professor with Bohai University. His current research interests include event-triggered control, intelligent control and adaptive control for nonlinear systems.

Yingnan Pan received the B.S. degree in mathematics and applied mathematics and the M.S. degree in applied mathematics from Bohai University, Jinzhou, China, in 2012 and 2015, respectively, and the Ph.D. degree in navigation guidance and control from Northeastern University, Shenyang, China, in 2019. He is currently an associate professor with Bohai University, Jinzhou, China. His current research interests include fuzzy control, adaptive control, event-triggered control and their applications.

Wenbin Xiao received the Ph. D. degree in control science and engineering from the Guangdong University of Technology, Guangzhou, China, in 2022. She is currently working with the School of Information and Electrical Engineering, Hunan University of Science and Technology, Xiangtan, China. Her research interests include distributed control, adaptive neural network control, and adaptive fuzzy control.

Hong Xue received the B.S. degree in mathematics from Bohai University, Jinzhou, China, in 2009, the M.S. degree in system theory from the Institute of Complexity Science, Qingdao University, Qingdao, China, in 2012. She is currently a lecturer with the Bohai University, Jinzhou, China. Her research interests include adaptive control, fuzzy control and their applications.